Marine phosphate level during the Archean constrained by the global redox budget

Yasuto Watanabe[1,2*], Kazumi Ozaki[3,4], Eiichi Tajika[1]

[1]Department of Earth and Planetary Science, The University of Tokyo, Tokyo, Japan

[2]Meteorological Research Institute, Japan Meteorological Agency, Tsukuba, Ibaraki, Japan

[3]Department of Earth and Planetary Sciences, Tokyo Institute of Technology, Tokyo, Japan

[4]Earth-Life Science Institute, Tokyo Institute of Technology, Meguro-ku, Tokyo, Japan

[*]Corresponding author: Yasuto Watanabe (yasuto.watanabe.wess@gmail.com)

Key Points:

- The marine phosphate levels on early Earth after the evolution of oxygenic photosynthesis is estimated using a theoretical model.
- Phosphate-rich oceans cause atmospheric oxygenation under reasonable outgassing rates of reducing gases and ocean circulation rate.
- Without suitable conditions, absence of oxygenic photosynthesis would be required for the phosphate-rich oceans during the Archean.

Abstract

Understanding the oceanic phosphate concentration is critical for understanding marine productivity and oxygen evolutions throughout Earth history. During the Archean, estimates of marine phosphate levels range from depleted to enriched conditions. However, biogeochemical conditions required for sustaining high phosphate concentrations while retaining an anoxic atmosphere during the Archean remain ambiguous. Here, we employ a biogeochemical model of the marine phosphate cycle to determine the conditions under which oceanic phosphate levels could have been higher than present-day values during the Archean after the emergence of oxygenic photoautotrophs. We show that, under the presence of oxygenic photoautotrophs, phosphate-rich oceans require the limitation by factors other than phosphate, or a combination of ocean stagnation and a high outgassing rate of reducing gases. If these conditions were not met, the occurrence of oceanic phosphate levels higher than present-day values during the Archean would require the absence of oxygenic photoautotrophs.

Plain Language Summary

The availability of phosphorus, a limiting nutrient in the ocean, is critical for understanding marine productivity in the history of the Earth, and hence atmospheric oxygen levels. On early Earth, the atmospheric oxygen level was much lower than the present conditions, and marine phosphate concentrations have been depleted. However, an emerging proxy of the past phosphate level indicates a phosphate-enriched condition, which may contradict with low atmospheric oxygen levels. To reveal the conditions required for sustaining high phosphate concentrations while retaining an anoxic atmosphere, we employed a theoretical model of the marine phosphate cycle. We show that, if oxygenic photosynthesis has evolved on early Earth, the primary productivity needs to be limited by factors other than phosphorus, such as nitrogen, or conditions with very slow ocean circulation and a high outgassing rate of reducing gases from volcanoes for achieving high marine phosphate concentrations. If these conditions were not met, phosphate-rich conditions on early Earth would be limited to the periods before the evolution of oxygenic photosynthesis.

1 Introduction

The mass-independent fractionation of sulfur isotopes (S-MIF) in sedimentary rocks recorded during the Archean (4.0–2.5 Ga) indicates an anoxic atmosphere with an oxygen partial pressure (pO_2) 10^{-6} times smaller than the present atmospheric level (PAL) until the first rise of atmospheric pO_2–the Great Oxidation Event (GOE)–at ~2.5–2.2 Ga (Farquhar et al. 2000; Pavlov and Kasting 2002; Lyons et al. 2014; Catling and Zahnle 2020). Despite this low atmospheric pO_2, accumulating geological records of the transient oxygenation of the ocean–atmosphere system (Anbar et al. 2007; Garvin et al. 2009; Czaja et al. 2012; Crowe et al. 2013;

Planavsky et al. 2014; Stüeken et al. 2015a; Ossa Ossa et al. 2016, 2018; Koehler et al. 2018) and phylogenetic analyses of cyanobacteria and O_2-utilizing and -producing enzymes (Schirrmeister et al. 2015; Garcia-Pichel et al. 2019; Jabłońska and Tawfik 2021) infer the emergence of oxygenic photoautotrophs (OP) by the middle Archean. If true, this indicates that the rate of biogenic O_2 supply must have been overwhelmed by the removal flux of O_2 (e.g., via the input of reducing species) for a sustained period of time.

The suppression of nutrient (i.e., phosphorus; P) availability in the ocean has been proposed as one plausible reason for sustained anoxic conditions throughout the Archean. Phosphorus, a bioessential element for life on Earth, is considered to be an ultimate limiting nutrient (Tyrrell 1999), which controls the global productivity of marine ecosystems on geological timescales. Geochemical analyses of Fe and P abundances in Archean iron formations (IF) indicate a low P availability (Bjerrum and Canfield 2002; Jones et al. 2015; Rego et al. 2023), although the estimated phosphate concentrations would be affected by uncertainties in the concentrations of cations such as Si^{2+}, Mg^{2+}, and Ca^{2+} (Konhauser et al. 2007; Jones et al. 2015). Records of P abundance in shales also support a condition of P scarcity during the Archean (Planavsky et al. 2014; Reinhard et al. 2017). The P scarcity is also supported by biogeochemical models (Reinhard et al. 2017; Kipp and Stüeken 2017; Watanabe et al. 2023a).

However, in contrast to previous studies, recent studies suggest the possibility that oceanic phosphate levels during the Archean were comparable to or higher than today (Konhauser et al. 2007; Planavsky et al. 2010; Rasmussen et al. 2021, 2023; Ingalls et al. 2022; Crockford and Halevy 2022). Records of P/Ca ratios in shallow marine carbonate minerals (carbonate-associated phosphate, CAP) at ~2.8–2.5 Ga suggest phosphate-rich oceans with 4–12 times higher phosphate concentrations compared with the present day (Ingalls et al. 2022).

Maximum phosphate concentrations of 10–100 μM are inferred from records of apatite nanoparticles with greenalite in deep-water banded IF deposited between 3.46 and 2.46 Ga (Rasmussen et al. 2021). Records of the co-precipitation of Ca-phosphate and ferrous silicate infer a P concentration several orders of magnitude higher than that in the present-day photic zone at 2.46–2.40 Ga (Rasmussen et al. 2023). These contradicting views of phosphate levels in the Archean oceans highlight a lack of quantitative understanding of the P cycle in the geological past. In this study, we examine the possibility that oceanic phosphate levels were higher than today during the Archean after the emergence of OP using a biogeochemical model of marine P cycle together with a global Fe and redox (O_2) budget.

2 Materials and Methods

We constructed a conceptual biogeochemical box model that simulates the global P cycle considering the global Fe and O_2 budgets (Figure 1). In this framework, the condition for low atmospheric pO_2 can be represented by the principle of the global redox budget (Claire et al. 2006; Watanabe et al. 2023b). The K_{oxy} value is used to measure the condition for the oxygenation of the atmosphere:

$$K_{oxy} = \frac{2F_{bg}}{F_{red}+0.5F_{oxfe}}, \quad (1)$$

where, F_{bg} is the burial flux of organic carbon (OC), F_{red} represents the volcanic outgassing rate of reducing gasses (in terms of Tmol H_2 eq. yr^{-1}), and F_{oxfe} is the deposition rate of Fe(III) hydroxides. Note that the weighting factor scales the effect of the burial of OC and Fe(III) in terms of the reducing power of H_2. When K_{oxy} is below unity, the rapid sink terms of O_2 outweigh the source of O_2, hindering the build-up of O_2 in the atmosphere (Claire et al. 2006; Watanabe et al. 2023b). We note here that oxidative weathering of continental crust and hydrogen escape do not appear in Equation 1 because these terms would be very small at the

boundary of the abrupt rise of pO_2 (Claire et al. 2006; Kasting 2013; Watanabe et al. 2023b). When K_{oxy} reaches unity, the oxygenation of the atmosphere (i.e., the GOE) occurs. In other words, the conditions for achieving an oxic atmosphere can be represented as follows:

$$F_{bg} = \frac{1}{4}(F_{oxfe} + 2F_{red}). \quad (2)$$

Note that, in the above equations, we do not consider the effect of pyrite burial for the purpose of obtaining upper estimates of marine phosphate concentrations because pyrite burial promotes oxygenation of the atmosphere. The P deposition as vivianite is also ignored for the purpose of obtaining a maximum estimate of marine phosphate concentrations. With these assumptions, the external supply rate of Fe(II) ($F_{ext,fe}$) is equal to F_{oxfe}:

$$F_{ext,fe} = F_{oxfe}. \quad (3)$$

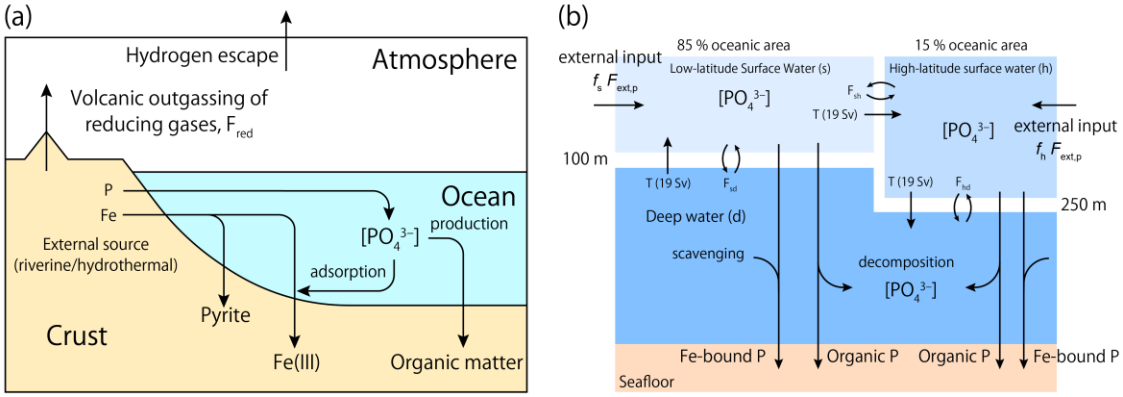

Figure 1. Schematic illustration of the global redox budget during the Archean (a) and an illustration of the biogeochemical box model used in this study (b).

For marine P cycles, we constructed a biogeochemical model with three ocean boxes (Figure 1b). The model is composed of the low-latitude surface ocean box (*s*), high-latitude surface ocean box (*h*), and deep ocean box (*d*). The marine P budget in the whole ocean is represented as follows:

$$F_{ext,p} = F_{bg,p} + F_{scav,p}, \quad (4)$$

where $F_{ext,p}$ denotes the external input flux of P to the ocean, $F_{bg,p}$ is the burial rate of phosphorus in marine sediments, and $F_{scav,p}$ represents the P removal flux via scavenging by Fe minerals from the ocean. The export production of organic P ($F_{po,p}$) and organic C (F_{po}) is determined by the phosphate concentration in the euphotic zone, $[PO_4^{3-}]_i$ (Yamanaka and Tajika 1996; Ozaki et al. 2019a; Watanabe et al. 2023a):

$$F_{po,p,i} = \epsilon_i \cdot [PO_4]_i \cdot V_{pz,i} \cdot \frac{[PO_4]_i}{[PO_4]_i + \gamma_p}, \quad (i = s, h) \quad (5)$$

$$F_{po} = (C_{bio}:P_{bio}) \cdot (F_{po,p,s} + F_{po,p,h}) \quad (6)$$

where V_{pz} denotes the volume of the photic zone of the surface water boxes; C_{bio}:P_{bio} represents the C:P ratio of the marine organic matter; γ_p is the half-saturation constant for the export production ($\gamma_p = 1.0 \times 10^{-6}$ mol L^{-1}); and ε is the efficiency factor for phosphorus uptake (ε_s and ε_h are 3.0 and 0.8 yr^{-1}, respectively), which is tuned to represent the present oceanic P concentration (Figure S1). The burial rate of organic C and P (F_{bg} and $F_{bg,p}$, respectively) is represented as follows:

$$F_{bg} = \alpha_d \cdot F_{po} \quad (7)$$

$$F_{bg,p} = \frac{1}{(C_{org}:P_{reac})} \cdot F_{bg} \quad (8)$$

where α_d is the ratio between burial rate of organic carbon and export production rate, and C_{org}:P_{reac} represents the C_{org}: reactive P (originating from organic P) ratio of buried sediments. The value of α_d is set to 20%, so that the burial rate of OC relative to the primary production rate

is the same as the modern value of the Black Sea (2%) (Betts and Holland 1991) where the bottom water is anoxic and sulfidic. It should be noted that the ratio of export production rate from the surface ocean and the primary production rate of 10% is assumed following the previous study (α_d = 0.02/0.10 = 0.20) (Ozaki et al. 2019a; Watanabe et al. 2023a). In the Archean ocean, this value is highly uncertain (Kuntz et al. 2015; Kipp and Stüeken 2017; Laakso and Schrag 2018; Ozaki et al. 2018; Kipp et al. 2020) because it may be much higher than this value owing to the lack of sulfate ions (Kuntz et al. 2015; Laakso and Schrag 2018). Nevertheless, our lower value allows us to obtain the maximum estimate of the marine phosphate concentrations that can be achieved on early Earth. C_{org}:P_{reac} is treated as a constant (the standard value is assumed to be 200) (Algeo and Ingall 2007), and the impact of its uncertainty on the results is examined in sensitivity experiments. We note here that the Ca-bound P burial, the primary P removal pathway in the present ocean, is not explicitly considered but its effect is represented by the factor C_{org}:P_{reac} assuming that the Ca-bound P originates from the buried organic P.

To get the steady-state solution with the constraint of K_{oxy} of 1, the model is run with the following external P supply rate:

$$F_{ext,p} = F_{bg,p,steady} + F_{scav,p} \quad (9)$$

where $F_{bg,p,steady}$ is the burial rate of phosphorus in marine sediments at a steady state calculated using equation 1. The marine phosphate concentration converges into a steady state that achieves K_{oxy} = 1. We estimated the response of the marine P concentration to the oceanic overturning rate and other parameters that potentially affect the result (Table S1). The values of the standard parameters are summarized in Table S2, which reproduces the present oceanic P concentrations (Figure S1).

3 Results

3.1 Constraints from low atmospheric pO_2 during the Archean

The relationship between the K_{oxy} value and $[PO_4^{3-}]_d$ is shown in Figure 2a. Different lines represent the results with different $F_{ext,fe}$ values (0, 1, 10, and 100 Tmol Fe yr^{-1}). These calculations are conducted with F_{red} of 10 Tmol H_2 eq. yr^{-1}. In any $F_{ext,fe}$ value, the estimated $[PO_4^{3-}]_d$ increases when K_{oxy} increases because high K_{oxy} values represent a high burial rate of OC (Figure 2b). When K_{oxy} exceeds 1, an abrupt increase of atmospheric pO_2 corresponding to GOE must occur (Claire et al. 2006; Kasting 2013; Watanabe et al. 2023b, a). At this boundary, $[PO_4^{3-}]_d$ is ~0.1 μM (~5% of the present oceanic level; POL) when $F_{ext,fe}$ is zero (Figure 2a). This value is an upper limit of the $[PO_4^{3-}]_d$ value under a given $F_{ext,fe}$ when the atmospheric pO_2 is low as in the Archean atmosphere. This maximum $[PO_4^{3-}]_d$ value becomes even lower when $F_{ext,fe}$ increases. As $F_{ext,fe}$ increases, the threshold value of F_{bg} required for the inception of the GOE increases because the oxygenation of Fe(II) prevents the oxygenation of the atmosphere.

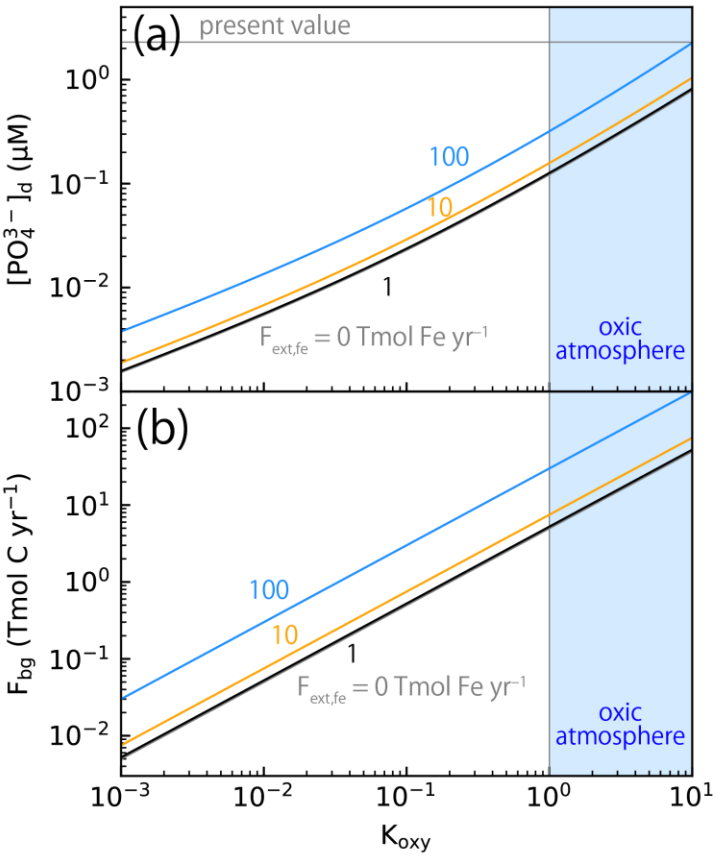

Figure 2. Relationships between K_{oxy} and marine P concentration (a) and the burial flux of organic carbon (b) (*ExpKoxy* in Table S1). The grey, black, orange, and light blue lines represent the results with $F_{ext,fe}$ of 0, 1, 10, and 100 Tmol Fe yr^{-1}. The blue-hatched region represents the condition for the oxic atmosphere ($K_{oxy} \geq 1$). We note here that the results with $F_{ext,fe}$ of 0 and 1 are very close.

The estimated maximum $[PO_4^{3-}]_d$ (corresponding to a value for K_{oxy} = 1) is summarized in a parameter space of $F_{ext,fe}$ and F_{red} in Figure 3a. The orange line represents the present $[PO_4^{3-}]_d$. The relationship between the Fe(II) influx and burial rate of OC at the boundary of the oxygenation of the atmosphere (i.e., K_{oxy} = 1) with different F_{red} values is shown in Figure 3b. The required F_{bg} for the GOE becomes higher for larger values of F_{red} and $F_{ext,fe}$. When F_{red} is small (<~10 Tmol H_2 eq. yr^{-1}), the $[PO_4^{3-}]_d$ value is still more than one order of magnitude smaller than the present condition. With an F_{red} of 1 Tmol H_2 eq. yr^{-1}, for example, $[PO_4^{3-}]_d$ is less than 1 μM (approximately 40% POL) even under extremely high $F_{ext,fe}$ (1000 Tmol Fe yr^{-1}). This range is consistent with the estimates of a P-scarce ocean (Jones et al. 2015; Kipp and Stüeken, 2017; Reinhard and Planavsky 2022; Rego et al. 2023; Watanabe et al. 2023a) (black line in Figure S2C) and it also allows the plausible range of estimates from CAP records (Ingalls et al. 2022; Crockford and Halevy 2022), but the maximum value is still much lower than other estimates of P-rich conditions (Planavsky et al. 2010; Rasmussen et al. 2021, 2023). To achieve such P-rich oceans (>100% POL), the outgassing rate of reducing gases must be very high. Specifically, when the outgassing rate of F_{red} is very high (>300 Tmol H_2 yr^{-1}), $[PO_4^{3-}]_d$ higher than the present value could be achieved while maintaining an anoxic atmosphere. These results demonstrate that if the activity of OP is limited by P availability, an extremely elevated outgassing rate of reducing gases is required for deep-ocean P concentrations to be similar to, or more enriched than, those of the present ocean while keeping the ocean–atmosphere system anoxic.

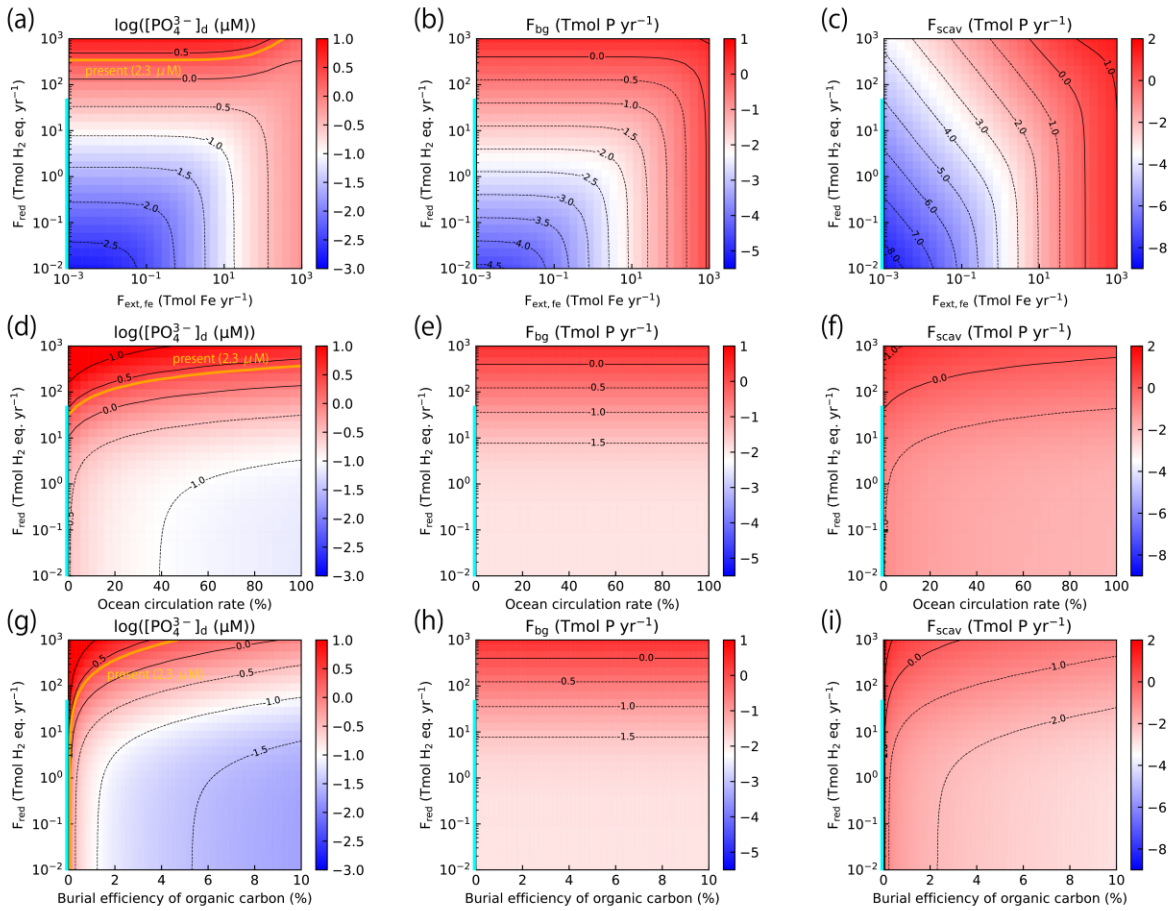

Figure 3. Estimated marine P concentrations (a, d, and g), burial flux of organic carbon (b, e, and h), and scavenging flux of P from the ocean (c, f, and i) shown as a parameter space of the Fe(II) influx ($F_{ext,fe}$) and the reducing gas influx (F_{red}) (*ExpFextfeFred* in Table S1) (a–c), the ocean circulation rate relative to the present condition and F_{red} (*ExpCircFred* in Table S1) (d–f), and the burial efficiency of organic carbon and F_{red} (*ExpBurFred* in Table S1) (g–i). The burial efficiency of organic carbon is changed by changing α_d while fixing the export production efficiency at 10%. The cyan bars represent the range below the maximum value of F_{red} in Krissansen-Totton et al. (2018). The orange lines in a, d, and g represent the condition for the present marine P concentration. Calculations are conducted under the condition of K_{oxy} of 1.

Constraints from the influx of reducing gases

The conditions for the oxygenation of the atmosphere are shown in a diagram of the marine phosphate concentration and influx of reducing power to the ocean–atmosphere system (F_{red} + 0.5 $F_{ext,fe}$) (Figure 4). The pink-hatched region represents the maximum outgassing rate from serpentinization of the oceanic crust considering the uncertainty in crustal production rates and FeO content in the oceanic crust (~50 Tmol H_2 eq. yr^{-1}) (Krissansen-Totton et al. 2018) (see their figure 6). Below this maximum F_{red}, the marine phosphate concentration is 0.5 μM (~20% POL). When F_{red} is extremely high, way beyond the maximum value, the present marine phosphate concentration could be achieved while keeping the atmosphere anoxic, implying that phosphate-rich conditions require an unrealistically high influx of reducing gases. To confirm the robustness of this result, the effects of uncertainties in other model parameters were also examined (Figure 3d–3i and Figure S3). The uncertainty related to the scavenging of P from the ocean by Fe hydroxides does not strongly affect the possible maximum $[PO_4^{3-}]_d$ (Figure S3). This is because the effective P scavenging decreases the K_{oxy} value in the Archean ocean, while we are exploring the $[PO_4^{3-}]_d$ when K_{oxy} is 1. It should be noted that, despite its small impact on $[PO_4^{3-}]_d$ when K_{oxy} is 1, P scavenging would decrease K_{oxy} and $[PO_4^{3-}]_d$ to lower values, limiting the achievement of high P (Bjerrum and Canfield 2002; Ozaki et al. 2019b; Watanabe et al. 2023a). In contrast, the sensitivity experiment with respect to the oceanic overturning rate (Figure 3d–3f and S3b), demonstrates that stagnant ocean circulation could allow a higher $[PO_4^{3-}]_d$. Specifically, when the oceanic overturning rate is < 25% of the standard value, $[PO_4^{3-}]_d$ of >100% POL is permissible assuming the maximum F_{red}, which may explain the reconstructions of Ingalls et al. (2022). However, the range of the influx of reducing gases required for sustaining the present marine P concentration is rather limited (Figure 3d). This result

demonstrates that marine P concentrations higher than the present condition cannot be achieved without extremely high influxes of reducing power.

The condition for achieving high marine P would even become more severe when a higher value for the burial efficiency of organic carbon in the ocean. We assumed a burial efficiency of the Black Sea as a lower limit for the Archean ocean, but existing literature indicates a higher burial efficiency (Kuntz et al. 2015; Laakso and Schrag 2018). With a higher burial efficiency of organic carbon, the F_{red} value required for $[PO_4^{3-}]_d$ of >100% POL becomes even higher. For the case with the burial efficiency of organic carbon of 10%, $[PO_4^{3-}]_d$ of 100% POL cannot be achieved even with F_{red} of 1000 Tmol H_2. eq. yr^{-1}. These results indicate the difficulty of achieving high marine P concentrations under the existence of OP.

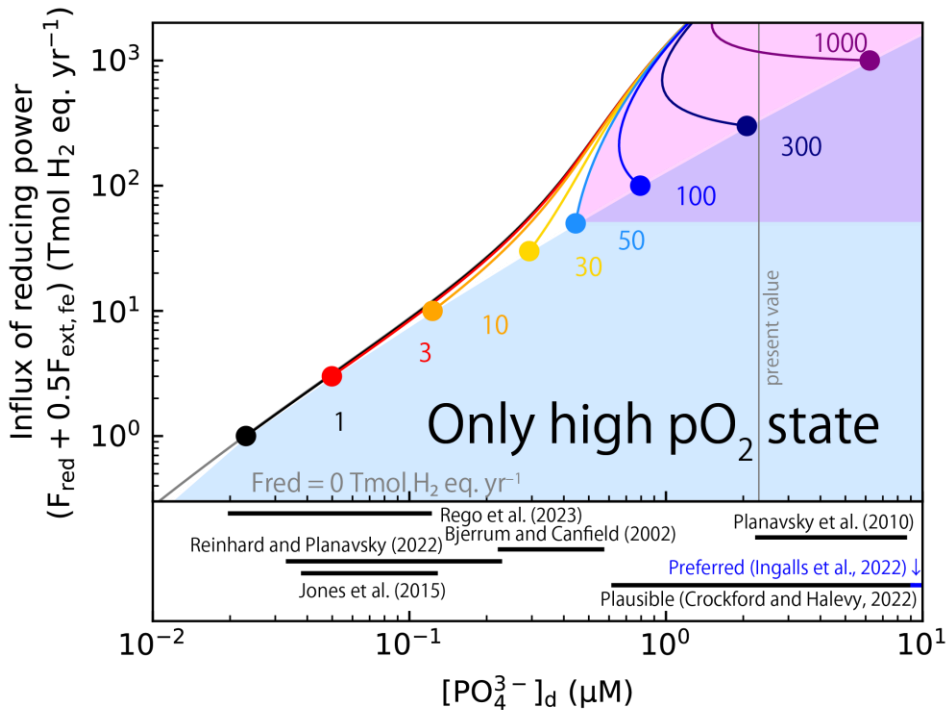

Figure 4. Relationships between the marine phosphate concentration calculated under a constraint of K_{oxy} of 1 (*ExpFextfe* in Table S1). The gray, black, red, orange, yellow, light blue, blue, navy, and purple lines represent sets of results with outgassing rates of reduced gases of 0, 1, 3, 10, 30, 50, 100, 300, and 1000 Tmol H_2 eq. yr^{-1}, respectively. The pink-hatched region is the condition that requires influxes of reducing gases greater than the maximum value for serpentinization of the oceanic crust. The estimates of the Archean marine P are summarized in Crockford and Halevy (2022).

4 Discussion

Our results demonstrate that marine phosphate concentrations >100% POL are limited to the condition of an unrealistically high influx of reduced gases larger than the maximum value for serpentinization of the oceanic crust (Krissansen-Totton et al. 2018), if the oceanic circulation rate is not stagnant (>25% of the modern value). This flux would be difficult to achieve on the early Earth even considering other sources of reducing gases; for example, the rate of H_2 release from the mantle is estimated at ~2.2 Tmol H_2 eq. yr^{-1} (Holland 1984; Catling and Kasting 2017) and this value may be even smaller considering the uncertainty regarding fluxes of H_2O and CO_2 (Catling and Kasting 2017). Reconstructions of the H_2 outgassing rate from Precambrian continental lithosphere give values of ~0.036–0.227 Tmol H_2 yr^{-1} (Lollar et al. 2014). These estimates are two or three orders of magnitude lower than the H_2 outgassing rate required for hypothetical P-rich oceans during the Archean. This clearly indicates that a high marine P concentration would be difficult to sustain during the Archean after the emergence of OP, if OP global activity is limited by P availability. It should be noted that if the oxygen fugacity in the Archean mantle is highly depleted, a higher outgassing flux may be possible (Wogan and Catling 2020; Wogan et al. 2020; Kadoya et al. 2020; Kipp et al. 2020; Krissansen-Totton et al. 2021). Nevertheless, the condition for high P concentration is rather limited as shown in Figure 3a. This may suggest that high marine P during the mid–late Archean indicates the absence of OP (Ingalls et al. 2022). Although phylogenetic analyses of cyanobacteria and O_2-utilizing and -producing enzymes infer the early emergence of OP (Schirrmeister et al. 2015; Garcia-Pichel et al. 2019; Jabłońska and Tawfik 2021), other studies suggest that the emergence of OP occurred immediately before the oxygenation of the atmosphere during the Paleoproterozoic (Kopp et al. 2005). If the latter is the case, O_2 was not generated during much of the Archean. Assuming that the activity of the anaerobic biosphere is limited by the supply rate of electron donors (e.g., H_2,

CO, H_2S, Fe(II), etc.), the primary productivity would be ~1% or less of the present productivity (Kharecha et al. 2005; Canfield et al. 2006; Ozaki et al. 2018). Because the amount of P required to sustain such a low activity level is small, high P concentrations could be achieved under an anoxic atmosphere in the absence of OP.

During the late Archean, geological records of transient oxygenation infer the presence of OP (Anbar et al. 2007; Garvin et al. 2009; Czaja et al. 2012; Crowe et al. 2013; Planavsky et al. 2014; Stüeken et al. 2015a; Ossa Ossa et al. 2016, 2018; Koehler et al. 2018). If this is the case, high marine P during the Archean would require the limitation of primary productivity by other factors, e.g., nitrogen, N. Before the evolution of nitrogenase—a N-fixing enzyme that allows N fixation—the availability of bioavailable N species in the ocean–atmosphere system would have been limited. If biospheric activity was limited by the availability of N (Kasting and Siefert 2001; Navarro-González et al. 2001), P would have accumulated to higher levels than those estimated under the assumption of a P-limited ecosystem. Indeed, a previous modeling study that implicitly assumes a limitation of primary productivity by the availability of N near the continental shelf indicates a marine P over 100% POL under a reasonable influx of reducing power (Alcott et al. 2019). We note that their model is based on the phosphorus cycle model of the present ocean (Slomp and Van Cappellen 2007), which assumes a linear relationship between P concentrations and the primary production in the proximal coastal ocean obtained for a condition with a N:P ratio of ~10 (lower than the Redfield's ratio (N:P ratio of 16) and thus N limitation) (Slomp and Van Cappellen 2004). This supports the feasibility of high P conditions under N-limited conditions. However, it has been proposed that the age of origin of nitrogenase was ~3.2 Ga (Stüeken et al. 2015b), which may suggest that P-rich reconstructions during the Archean require the absence of OP or limitations of primary productivity by other unconsidered

factors. One of the other factors that may limit the primary productivity of OP is the competition of P between the anoxygenic photoautotrophs, which can survive with weaker sunlight at a deeper part of the euphotic zone and thus has a priority in utilizing P upwelling from deep oceans (Ozaki et al. 2019b). This limitation would require a high Fe/P ratio in the deep ocean. Further investigation using a biogeochemical model with Fe and P dynamics would be a fruitful topic (Laakso and Schrag 2014; Watanabe et al. 2023a).

5 Conclusion

The biogeochemical conditions required for P-rich oceans during the Archean were examined. Our biogeochemical model revealed that oceanic phosphate concentrations higher than today would have been difficult to achieve during the Archean if OP had already evolved and their activity was limited by phosphate availability. Under such conditions, P-rich oceans would have given rise to the oxygenation of the atmosphere unless the input flux of reducing gases was unrealistically high or the ocean was stagnant. The P-rich oceans during the Archean would require the absence of OP or limitations of productivity by other factors (e.g., bioessential elements other than P). Further constraints on marine phosphate concentrations and behaviors of P in anoxic oceans would be beneficial for understanding marine biogeochemical cycles during the Archean.

Acknowledgments

This work is supported by Grant-in-aid for JSPS KAKENHI Grants Number 22H05150 (KO), JST FOREST Program (Grant Number JPMJFR22743, Japan) (KO), and Mitsubishi Foundation (202210014) (KO). We thank M. A. Kipp for providing constructive comments on the earlier draft. We thank David Wacey, PhD, from Edanz (https://jp.edanz.com/ac) for editing a draft of this manuscript.

Open Research

The data that reproduces the figues of this research are archived in the following repository:

https://zenodo.org/records/10511558

References

Alcott LJ, Mills BJW, Poulton SW (2019) Stepwise Earth oxygenation is an inherent property of global biogeochemical cycling. Science 366:1333–1337

Algeo TJ, Ingall E (2007) Sedimentary Corg:P ratios, paleocean ventilation, and Phanerozoic atmospheric pO2. Palaeogeogr Palaeoclimatol Palaeoecol 256:130–155

Anbar AD, Duan Y, Lyons TW, et al (2007) A whiff of oxygen before the great oxidation event? Science 317:1903–1906

Archer DE, Eshel G, Winguth A, et al (2000) Atmospheric pCO2 sensitivity to the biological pump in the ocean. Global Biogeochem Cycles 14:1219–1230

Berner RA (1973) Phosphate removal from sea water by adsorption on volcanogenic ferric oxides. Earth Planet Sci Lett 18:77–86

Betts JN, Holland HD (1991) The oxygen content of ocean bottom waters, the burial efficiency of organic carbon, and the regulation of atmospheric oxygen. Glob Planet Change 97:5–18

Bjerrum CJ, Canfield DE (2002) Ocean productivity before about 1.9 Gyr ago limited by phosphorus adsorption onto iron oxides. Nature 417:159–162

Bocher F, Géhin A, Ruby C, et al (2004) Coprecipitation of Fe(II–III) hydroxycarbonate green rust stabilised by phosphate adsorption. Solid State Sci 6:117–124

Canfield DE, Rosing MT, Bjerrum C (2006) Early anaerobic metabolisms. Philos Trans R Soc Lond B Biol Sci 361(1474), 1819–1836

Catling DC, Kasting JF (2017) Atmospheric evolution on inhabited and lifeless worlds. Cambridge University Press

Catling DC, Zahnle KJ (2020) The Archean atmosphere. Sci Adv 6:eaax1420

Claire MW, Catling DC, Zahnle KJ (2006) Biogeochemical modelling of the rise in atmospheric oxygen. Geobiology 4:239–269

Cosmidis J, Benzerara K, Morin G, et al (2014) Biomineralization of iron-phosphates in the water column of Lake Pavin (Massif Central, France). Geochim Cosmochim Acta 126:78–96

Crockford P, Halevy I (2022) Questioning the paradigm of a phosphate-limited Archean biosphere. Geophys Res Lett 49(17), e2022GL099818.

Crowe SA, Døssing LN, Beukes NJ, et al (2013) Atmospheric oxygenation three billion years ago. Nature 501:535–538

Czaja AD, Johnson CM, Roden EE, et al (2012) Evidence for free oxygen in the Neoarchean ocean based on coupled iron–molybdenum isotope fractionation. Geochim Cosmochim Acta 86:118–137

Farquhar J, Bao H, Thiemens M (2000) Atmospheric influence of Earth's earliest sulfur cycle. Science 289:756–759

Garcia-Pichel F, Lombard J, Soule T, et al (2019) Timing the Evolutionary Advent of Cyanobacteria and the Later Great Oxidation Event Using Gene Phylogenies of a Sunscreen. MBio 10(3), 10-1128.

Garvin J, Buick R, Anbar AD, et al (2009) Isotopic evidence for an aerobic nitrogen cycle in the latest Archean. Science 323:1045–1048

Holland HD (1984) The chemical evolution of the atmosphere and oceans. Princeton University Press.

Ingalls M, Grotzinger JP, Present T (2022) Carbonate-associated phosphate (CAP) indicates elevated phosphate availability in Neoarchean shallow marine environments. Geophysical Research Letters 49(6), e2022GL098100

Jabłońska J, Tawfik DS (2021) The evolution of oxygen-utilizing enzymes suggests early biosphere oxygenation. Nat Ecol Evol 5:442–448

Jones C, Nomosatryo S, Crowe SA, et al (2015) Iron oxides, divalent cations, silica, and the early earth phosphorus crisis. Geology 43:135–138

Kadoya S, Catling DC, Nicklas RW, et al (2020) Mantle data imply a decline of oxidizable volcanic gases could have triggered the Great Oxidation. Nat Commun 11:2774

Kasting JF (2013) What caused the rise of atmospheric O2? Chem Geol 362:13–25

Kasting JF, Siefert JL (2001) Biogeochemistry. The nitrogen fix. Nature 412:26–27

Kharecha P, Kasting J, Siefert J (2005) A coupled atmosphere-ecosystem model of the early Archean Earth. Geobiology 3:53–76

Kipp MA, Stüeken EE (2017) Biomass recycling and Earth's early phosphorus cycle. Sci Adv

3:eaao4795

Kipp M, Krissansen-Totton J, Catling DC (2020) High burial efficiency is required to explain mass balance in Earth's early carbon cycle. Global Biogeochem Cycles. 35(2).

Koehler MC, Buick R, Kipp MA, et al (2018) Transient surface ocean oxygenation recorded in the ~2.66-Ga Jeerinah Formation, Australia. Proc Natl Acad Sci U S A 115:7711–7716

Konhauser KO, Lalonde SV, Amskold L, Holland HD (2007) Was there really an Archean phosphate crisis? Science 315:1234

Kopp RE, Kirschvink JL, Hilburn IA, Nash CZ (2005) The Paleoproterozoic snowball Earth: a climate disaster triggered by the evolution of oxygenic photosynthesis. Proc Natl Acad Sci U S A 102:11131–11136

Krissansen-Totton J, Kipp MA, Catling DC (2021) Carbon cycle inverse modeling suggests large changes in fractional organic burial are consistent with the carbon isotope record and may have contributed to the rise of oxygen. Geobiology, 19(4), 342-363.

Krissansen-Totton J, Olson S, Catling DC (2018) Disequilibrium biosignatures over Earth history and implications for detecting exoplanet life. Sci Adv 4:eaao5747

Krom MD, Berner RA (1980) Adsorption of phosphate in anoxic marine sediments1. Limnol Oceanogr 25:797–806

Kuntz LB, Laakso TA, Schrag DP, Crowe SA (2015) Modeling the carbon cycle in Lake Matano. Geobiology 13:454–461

Laakso TA, Schrag DP (2018) Limitations on limitation. Global Biogeochem Cycles 32:486–496

Laakso TA, Schrag DP (2014) Regulation of atmospheric oxygen during the Proterozoic. Earth Planet Sci Lett 388:81–91

Lollar BS, Onstott TC, Lacrampe-Couloume G, Ballentine CJ (2014) The contribution of the Precambrian continental lithosphere to global H2 production. Nature 516:379–382

Lyons TW, Reinhard CT, Planavsky NJ (2014) The rise of oxygen in Earth's early ocean and atmosphere. Nature 506:307–315

Navarro-González R, McKay CP, Mvondo DN (2001) A possible nitrogen crisis for Archaean life due to reduced nitrogen fixation by lightning. Nature 412:61–64

Ossa Ossa F, Hofmann A, Vidal O, et al (2016) Unusual manganese enrichment in the Mesoarchean Mozaan Group, Pongola Supergroup, South Africa. Precambrian Res 281:414–433

Ossa Ossa F, Hofmann A, Wille M, et al (2018) Aerobic iron and manganese cycling in a redox-stratified Mesoarchean epicontinental sea. Earth Planet Sci Lett 500:28–40

Ozaki K, Reinhard CT, Tajika E (2019a) A sluggish mid-Proterozoic biosphere and its effect on Earth's redox balance. Geobiology 17:3–11

Ozaki K, Tajika E, Hong PK, et al (2018) Effects of primitive photosynthesis on Earth's early climate system. Nature Geoscience 11:55–59

Ozaki K, Thompson KJ, Simister RL, et al (2019b) Anoxygenic photosynthesis and the delayed oxygenation of Earth's atmosphere. Nat Commun 10:3026

Pavlov AA, Kasting JF (2002) Mass-independent fractionation of sulfur isotopes in Archean sediments: strong evidence for an anoxic Archean atmosphere. Astrobiology 2:27–41

Planavsky NJ, Asael D, Hofmann A, et al (2014) Evidence for oxygenic photosynthesis half a billion years before the Great Oxidation Event. Nat Geosci 7:283–286

Planavsky NJ, Rouxel OJ, Bekker A, et al (2010) The evolution of the marine phosphate reservoir. Nature 467:1088–1090

Rasmussen B, Muhling JR, Suvorova A, Fischer WW (2021) Apatite nanoparticles in 3.46–2.46 Ga iron formations: Evidence for phosphorus-rich hydrothermal plumes on early Earth. Geology 49:647–651

Rasmussen B, Muhling JR, Tosca NJ, Fischer WW (2023) Did nutrient-rich oceans fuel Earth's oxygenation? Geology 51:444–448

Rego ES, Busigny V, Lalonde SV, et al (2023) Low-phosphorus concentrations and important ferric hydroxide scavenging in Archean seawater. PNAS Nexus 2:gad025

Reinhard CT, Planavsky NJ (2022) The History of Ocean Oxygenation. Ann Rev Mar Sci 14:331–353

Reinhard CT, Planavsky NJ, Gill BC, et al (2017) Evolution of the global phosphorus cycle. Nature 541:386–389

Schirrmeister BE, Gugger M, Donoghue PCJ (2015) Cyanobacteria and the Great Oxidation Event: evidence from genes and fossils. Palaeontology 58:769–785

Slomp CP, Van Cappellen P (2004) Nutrient inputs to the coastal ocean through submarine groundwater discharge: controls and potential impact. J Hydrol 295:64–86

Slomp CP, Van Cappellen P (2007) The global marine phosphorus cycle: sensitivity to oceanic circulation. Biogeosciences 4:155–171

Stüeken EE, Buick R, Bekker A, et al (2015a) The evolution of the global selenium cycle: Secular trends in Se isotopes and abundances. Geochim Cosmochim Acta 162:109–125

Stüeken EE, Buick R, Guy BM, Koehler MC (2015b) Isotopic evidence for biological nitrogen fixation by molybdenum-nitrogenase from 3.2 Gyr. Nature 520:666–669

Tyrrell T (1999) The relative influences of nitrogen and phosphorus on oceanic primary production. Nature 400:525–531

Watanabe Y, Tajika E, Ozaki K (2023a) Evolution of iron and oxygen biogeochemical cycles during the Precambrian. Geobiology 21(6), 689-707.

Watanabe Y, Tajika E, Ozaki K (2023b) Biogeochemical transformations after the emergence of oxygenic photosynthesis and conditions for the first rise of atmospheric oxygen. Geobiology 21:537–555

Wogan NF, Catling DC (2020) When is Chemical Disequilibrium in Earth-like Planetary Atmospheres a Biosignature versus an Anti-biosignature? Disequilibria from Dead to Living Worlds. The Astrophysical Journal 892:127

Wogan N, Krissansen-Totton J, Catling DC (2020) Abundant Atmospheric Methane from Volcanism on Terrestrial Planets Is Unlikely and Strengthens the Case for Methane as a Biosignature. The Planetary Science Journal 1:58

Yamanaka Y, Tajika E (1996) The role of the vertical fluxes of particulate organic matter and calcite in the oceanic carbon cycle: Studies using an ocean biogeochemical general circulation model. Global Biogeochem Cycles 10:361–382

Zegeye A, Bonneville S, Benning LG, et al (2012) Green rust formation controls nutrient availability in a ferruginous water column. Geology 40:599–602